JOURNAL OF MATERIALS SCIENCE 26 (1991) 1808–1814

# Tensile creep behaviour of a fibre-reinforced SiC–$Si_3N_4$ composite

J. W. HOLMES
*Ceramic Composites Research Laboratory, Department of Mechanical Engineering and Applied Mechanics, University of Michigan Ann Arbor, MI 48109-2125, USA*

The tensile creep behaviour of a SiC-fibre–$Si_3N_4$-matrix composite was investigated in air at 1350 °C. The unidirectional composite, containing 30 vol% SCS-6 SiC fibres, was prepared by hot pressing at 1700 °C. Creep testing was conducted at stress levels of 70, 110, 150 and 190 MPa. An apparent steady-state creep rate was observed at stress levels between 70 and 150 MPa; at 190 MPa, only tertiary creep was observed. For an applied stress of 70 MPa, the steady-state creep rate was approximately $2.5 \times 10^{-10}\,s^{-1}$ with failure times in excess of 790 h. At 150 MPa, the steady-state creep rate increased to an average of $5.6 \times 10^{-8}\,s^{-1}$ with failure times under 40 h. The creep rate of the composite is compared with published data for the steady-state creep rate of monolithic $Si_3N_4$.

## 1. Introduction

Fibre-reinforced ceramic matrix composites are under development for use in advanced gas turbines, heat exchangers and aerospace structures. However, due to their recent development, very little is known about the creep behaviour of these materials. To date, only Abbe *et al.* [1] have investigated the creep behaviour of *fibre*-reinforced ceramics. In their work, Abbe *et al.* examined the flexural creep of a 0°–90° SiC-fibre–SiC-matrix composite processed by chemical vapour infiltration (hereafter referred to as CVI-$SiC_f$–SiC). The creep tests were conducted in vacuum. At 1200 °C, the steady-state creep rate of the CVI-$SiC_f$–SiC composite ranged from approximately $1.9 \times 10^{-9}\,s^{-1}$ at 70 MPa to $1.1 \times 10^{-8}\,s^{-1}$ at 100 MPa; at 1400 °C the creep rate increased to $1.1 \times 10^{-8}\,s^{-1}$ at 70 MPa and $2.8 \times 10^{-8}\,s^{-1}$ at 100 MPa. Although the stress sensitivity of creep rate was low, the steady-state creep rate of the composite is higher than the creep rate typically found for monolithic α-SiC [2–5]. The relatively high creep rate of the composite may be a consequence of the high porosity content of the SiC matrix ( $\approx 20\%$). Also, as noted by Wiederhorn and Hockey [5], Nicalon fibres (utilized in the CVI-$SiC_f$–SiC composite investigated by Abbe *et al.* [1]) have poor chemical stability at high temperatures.

The present work examines the *tensile* creep behaviour of a unidirectional SiC-fibre–$Si_3N_4$-matrix composite formed by hot-pressing (hereafter referred to as HP-$SiC_f$–$Si_3N_4$). The creep behaviour of the composite was investigated in *air* at stress levels above and below the monotonic proportional limit strength of the composite.

## 2. Experimental procedure

### 2.1. Material and specimen geometry

The composite system used in this investigation was comprised of 30 vol % SCS-6 SiC fibres [6, 7] in a $Si_3N_4$ matrix. The monofilament β-SiC SCS-6 fibres have a diameter of 142 μm. The matrix composition was: 93.75% Stark LC-12 $Si_3N_4$, 5.00% $Y_2O_3$ and 1.25% MgO (in wt %). The matrix powder had a nominal particle diameter of 0.5 μm. The composite was formed by a dry-powder lay up technique. Matrix consolidation was accomplished by hot-pressing at 1700 °C under an applied pressure of 70 MPa (in vacuum)*. After consolidation, the billet dimensions were approximately 125 × 125 × 15 mm.[3] The density of the hot-pressed billet was $3.15\,g\,cm^{-3}$, which is close to 98% of the theoretical density for this system. A micrograph showing the fibre distribution in the hot-pressed billet investigated is given in Fig. 1. Edge-loaded creep specimens (Fig. 2) were machined from the billet using diamond tooling. The overall specimen length was 114 mm, with a gauge length of 33 mm.

### 2.2. Experimental arrangement

Creep testing was conducted on an MTS 810 Material Test System equipped with self-aligning hydraulic grips. All testing was conducted in air. An induction heated SiC susceptor was used to heat the specimen gauge-section (see Fig. 3). The temperature at the centre of the gauge-section was maintained at 1350 ± 1 °C; the maximum difference in temperature measured between any two points along the gauge-section was 12 °C. At the start of each test, the specimen temperature was increased from 22 to 1350 °C at a

* Material processed by Textron Specialty Materials, Lowell, MA, USA.



0022–2461/91 $03.00 + .12 

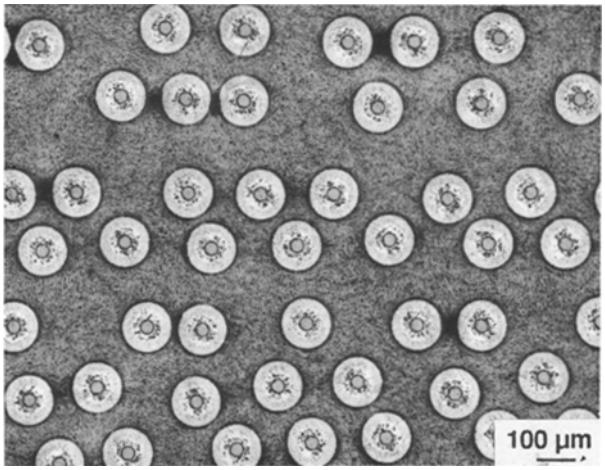


*Figure 1* SEM micrograph showing the typical fibre distribution in the hot-pressed $SiC_f$–$Si_3N_4$ billet studied.

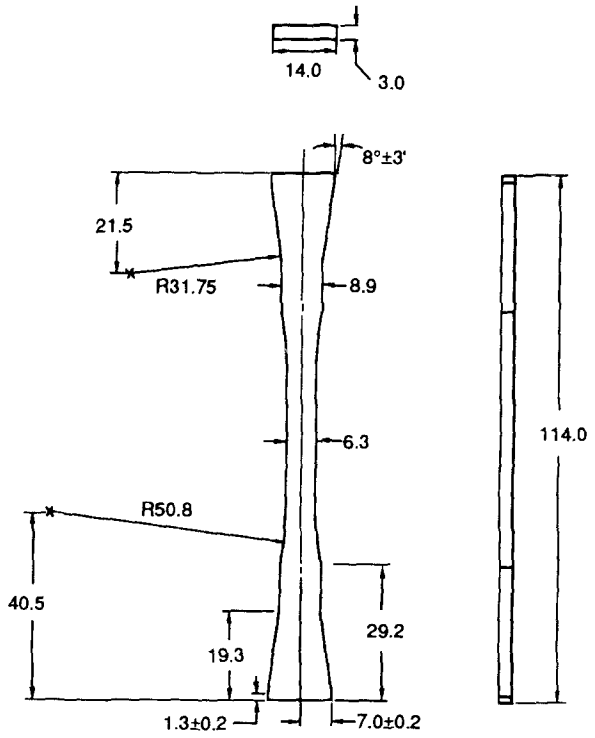


*Figure 2* Edge-loaded specimen used to investigate the tensile creep behaviour of HP $SiC_f$–$Si_3N_4$ composites. Dimensions in millimetres (unless shown otherwise, the tolerance on all dimensions was 0.1 mm).

linear rate of 50 °C $min^{-1}$. After reaching 1350 °C, the temperature of the furnace and specimen was allowed to equilibrate for 30 min before applying the creep load.

Specimen alignment, which is an important consideration in the testing of fibre-reinforced ceramics, was determined at 22 °C using the approach outlined in ASTM Standard E1012-84 [8]. For all loads used in creep testing, the maximum bending strain acting on the specimen was less than 1.8% of the axial strain. In addition to providing a stiff loading system with minimal bending strain, the servohydraulic test frame allowed accurate control over the initial loading rate of the creep specimens; for all tests, specimens were

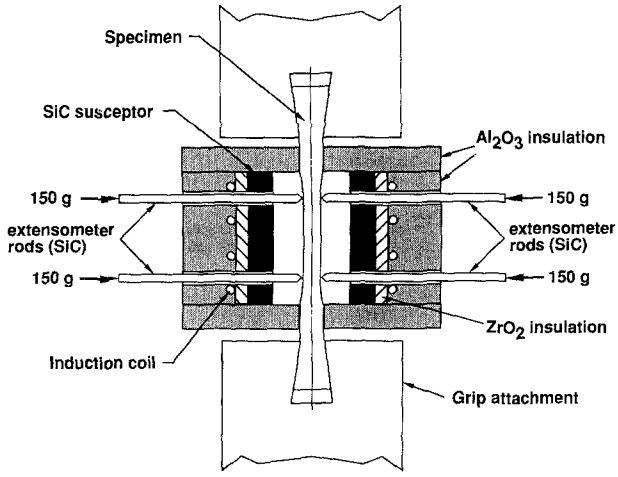


*Figure 3* Schematic of experimental arrangement used to study the tensile creep behaviour of HP-$SiC_f$–$Si_3N_4$. The grip attachments were machined from a Ni-base superalloy (Rene 80). To minimize the axial temperature gradient in the gauge-section of the specimen, the grip attachments were not cooled.

loaded to the desired creep stress at a rate of 100 MPa $s^{-1}$.

Creep strains were measured using two contact-type mechanical extensometers located on opposite sides of the specimen (see Fig. 3). As discussed in detail by Holmes *et al.* [9, 10], the use of two extensometers, in a counter-acting arrangement, allows using a moderate extensometer contact force without introducing bending strains in the specimen. Creep strains were determined by averaging the readings obtained from the two extensometers (the readings typically varied by less than 2% for all strain levels measured). Following the approach used for fatigue testing of a similar HP-$SiC_f$–$Si_3N_4$ composite [9, 11], the tips of the extensometer rods resided in small conical dimples which were ground into the edge of the specimen (this technique was found to be useful for preventing extensometer slip which can occur during tertiary creep, where considerable energy is expended during fracture of the fibers and matrix). In the present investigation, a contact force of 150 g per rod was utilized. By use of an alignment fixture it was verified that both extensometers loaded the specimen along the same plane. The extensometer and load cell signals were gathered by a data acquisition system with 16-bit resolution. During preliminary testing it was found that small temperature variations ( $\approx 3$ °C) in the room containing the experimental setup produced fluctuations in the strain readings. The fluctuations were traced to expansion and contraction of the portion of the extensometer rods which were external to the furnace (see Fig. 3). To minimize these fluctuations, the temperature in the vicinity of the test apparatus was maintained at $22 \pm 0.5$ °C.

## 2.3. Creep experiments

Prior to creep testing, the monotonic tensile behaviour of the composite was investigated to allow establishing appropriate stress levels for use in the creep

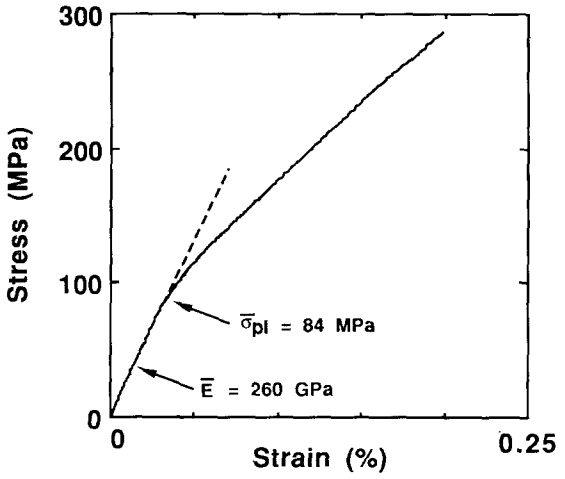


*Figure 4* Monotonic tensile response of HP-$SiC_f$–$Si_3N_4$ at 1350 °C.

experiments. At 1350 °C and a loading rate of 100 MPa $s^{-1}$ the composite exhibited an initially linear stress–strain response, followed by non-linear behaviour (see Fig. 4). Based upon the results obtained from four tensile tests, the onset of non-linear behaviour (hereafter referred to as the "proportional limit strength", $\sigma_{pl}$) began at 76 to 94 MPa; the average proportional limit strength was 84 MPa. The onset of non-linear behaviour during tensile loading of fibre-reinforced ceramics is typically attributed to the onset of significant matrix cracking or the extension of pre-existing flaws [12–18].* Microcracking can expose the fibre–matrix interface to oxygen in the test atmosphere, thus, the creep behaviour of the composite was investigated at stress levels above and below the proportional limit strength. Using the average proportional limit strength of 84 MPa as a reference, creep testing was conducted at stress levels of 70, 110, 150 and 190 MPa. To provide an indication of the variability in the creep data, three specimens were tested to failure at each stress level.

## 3. Experimental results and discussion

### 3.1. Creep behaviour

As the proportional limit can vary from specimen to specimen, the stress–strain behaviour of each specimen was determined during initial application of the creep load (this allowed verifying that specimens were, as desired, loaded to a stress level above or below $\sigma_{pl}$). Analysis of the initial stress–strain curves obtained from the specimens crept at 110, 150 and 190 MPa showed that the proportional limit of these samples ranged from 80 to 103 MPa, in good agreement with the range of 76 to 94 MPa found from monotonic tensile testing. The initial stress-strain curves obtained for the specimens crept at 70 MPa were linear; thus, for these samples little, if any, microcracking would have been present prior to creep testing.

The creep behaviour of the composite at 1350 °C is shown in Fig. 5 for stress levels of 70, 110 and 150 MPa. For these stress levels an apparent steady-state creep regime was observed, with primary and tertiary creep typically accounting for less than 20% of the total creep life. At 190 MPa, ( $\approx$ 65% of the monotonic tensile strength of the composite), only tertiary creep was observed, with failures occurring in under 5 min.

The stress dependence of the apparent steady-state creep rate is shown in Fig. 6 (a summary of failure times and corresponding failure strains are given in Table I). Under an applied stress of 70 MPa, ( $\approx$ 25% below the monotonic proportional limit of the composite), the steady-state creep rate ranged from 1.9 $\times$ $10^{-10}$ to 3.9 $\times$ $10^{-10}$ $s^{-1}$, with failure times between 794 and 975 h. Above the monotonic proportional limit, the average steady-state creep rate increased to an average of 1.0 $\times$ $10^{-8}$ $s^{-1}$ at 110 MPa

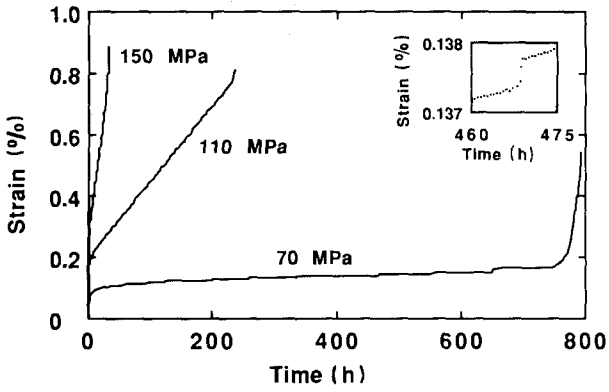


*Figure 5* Tensile creep behaviour of HP-$SiC_f$–$Si_3N_4$ at 1350 °C. Representative creep curves for stress levels of 70, 110 and 150 MPa are shown (at 190 MPa, only tertiary creep was observed, with failure occurring in under 5 min). The inset shows a typical strain jump observed during creep testing at 70 MPa.

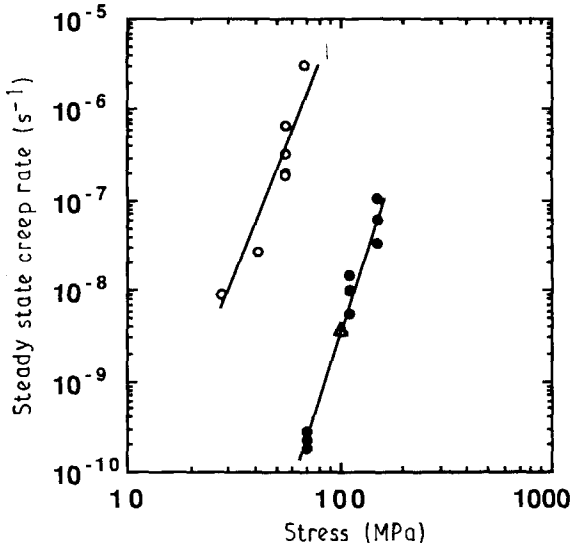


*Figure 6* Steady-state tensile creep rate plotted against stress for HP-$SiC_f$–$Si_3N_4$ at 1350 °C (•), monolithic HP-$Si_3N_4$ at 1315 °C [19] (○) and monolithic HIP-$Si_3N_4$ at 1370 °C [23] (△).

* When defined in this manner, initial microcracking, which was not sufficient in extent to produce a detectable change in specimen compliance (within the resolution of the extensometer) could have initiated at lower stress levels.

and $6.7 \times 10^{-8}\ s^{-1}$ at 150 MPa (corresponding failure times ranged from 190 to 282 h at 110 MPa and 22 to 40 h at 150 MPa). Fitting the steady-state creep rate data given in Fig. 6 to a power law ($\dot{\varepsilon}_{ss} \propto \sigma^n$) yields a stress exponent of approximately 7 for the HP-$SiC_f$–$Si_3N_4$ composite. Although this is a high stress exponent, it is comparable to the stress exponents of approximately 4 to 6 found for the tensile creep of monolithic [19–21] and whisker-reinforced $Si_3N_4$ [22].

In tension–tension fatigue testing of unidirectional HP-$SiC_f$–$Si_3N_4$ composites at 1000 and 1200 °C [9, 11], a sharp decrease in fatigue life was observed when the maximum fatigue stress exceeded the monotonic proportional limit of the composite, thus, it was anticipated that the matrix cracking which occurs at stress levels above the proportional limit would significantly influence the creep rate and time to failure; however, the data obtained from the present study (Fig. 6) show no significant change in creep rate (beyond that which is attributed to a change in stress alone) for stress levels above the proportional limit. Moreover, for stresses between 70 and 150 MPa ($\approx 0.8$ to $1.8\sigma_{pl}$) an approximately linear relationship exists between $\log \dot{\varepsilon}_{ss}$ and $\log \sigma_{creep}$, suggesting that the mechanism of creep damage does not change over this limited range of stress. Unfortunately, additional specimens were not available to determine if a similar stress dependence of creep rate would hold at stress levels substantially below the monotonic proportional limit. The apparent insensitivity of creep rate to the presence of microcracks formed during initial loading above the proportional limit may be related to the formation of a complex glass layer ($SiO_2$–$Y_2O_3$–MgO) which was found on the surface of all creep specimens (see Fig. 7). This glass layer, formed by oxidation of $Si_3N_4$ and sintering aids, may act to slow the degradation of fibres exposed to the test atmosphere through microcracking (in contrast, fatigue loading would disrupt the formation of a protective glass layer). In addition to the formation of an adherent glass layer on the specimen surface, a $SiO_2$-rich glass was occasionally observed within matrix cracks which formed in the gauge-section.

TABLE I Time to failure ($t_f$) and total strain at failure ($\varepsilon_f$) found for tensile creep testing of unidirectional HP-$SiC_f$–$Si_3N_4$ composites at 1350 °C (in air).

| Stress (MPa) | $t_f$ (h) | $\varepsilon_f$ (%) |
|---|---|---|
| 190 | 0.02 | 0.26 |
| | 0.04 | 0.34 |
| | 0.08 | 0.31 |
| 150 | 22.1 | 0.61 |
| | 34.0 | 0.88 |
| | 39.9 | 0.94 |
| 110 | 190.2 | 0.50 |
| | 236.4 | 0.81 |
| | 282.1 | 0.72 |
| 70 | 794.3 | 0.54 |
| | 847.7 | 0.67 |
| | 975.4 | 0.48 |

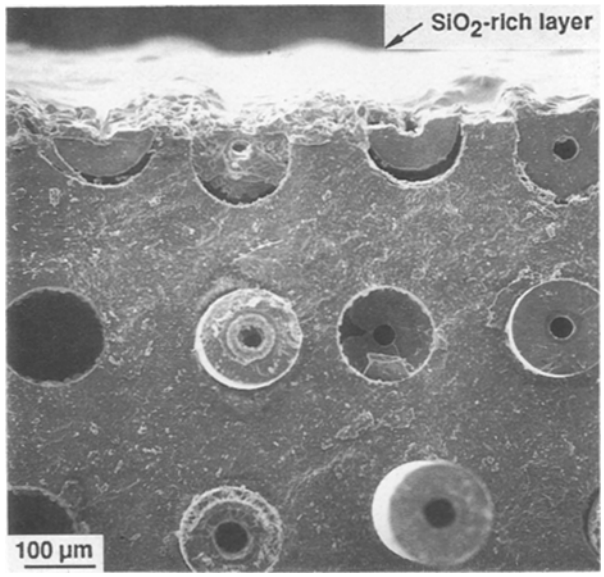


*Figure 7* SEM micrograph showing the formation of a glass layer on the surface of HP-$SiC_f$–$Si_3N_4$ specimens crept at 1350 °C (110 MPa, $t_f$ = 282.1 h). The micrograph was taken perpendicular to the fracture surface.

During creep at 70 and 110 MPa, instantaneous strain jumps were observed during "steady-state" creep. The instantaneous nature of these strain jumps was discernable only when the creep curves were examined on a much finer scale (see inset in Fig. 5). Each strain jump produced a gauge-section extension of approximately 1 to 2 μm. The increase in creep rate following each strain jump was typically less than 1% of the creep rate which immediately preceded a given strain jump. A possible mechanism for the discontinuous strain jumps, which is consistent with the instantaneous increase in gauge-section strain, would be the random fracture of individual fibres (discussed in greater detail below). It must be noted, however, that a similar effect could be explained by the increase in specimen compliance which would accompany the formation or extension of matrix cracks, followed by arrest at the fibres*. The discontinuous nature of the strain jumps offer evidence that irreversible microstructural damage accumulates during creep of the composite.

## 3.2. Microstructural observations

For the long duration creep tests ($\sigma_{creep}$ = 70 MPa), creep failures were accompanied by extensive fibre pullout. At 70 MPa, the length of the exposed fibres measured after failure varied from 0 to 6 mm (Fig. 8a). As the applied stress was increased, the extent of fibre pullout decreased (Fig. 8b); for example, at 150 MPa, the maximum pullout length of fibres was under 1 mm

* The possibility that extensometer slip or random electrical noise was responsible for the discontinuous strain jumps was ruled out after a series of calibration experiments, conducted for 400 h at 1350 °C and an applied stress of 2 MPa, showed continuous load cell and extersometer data.

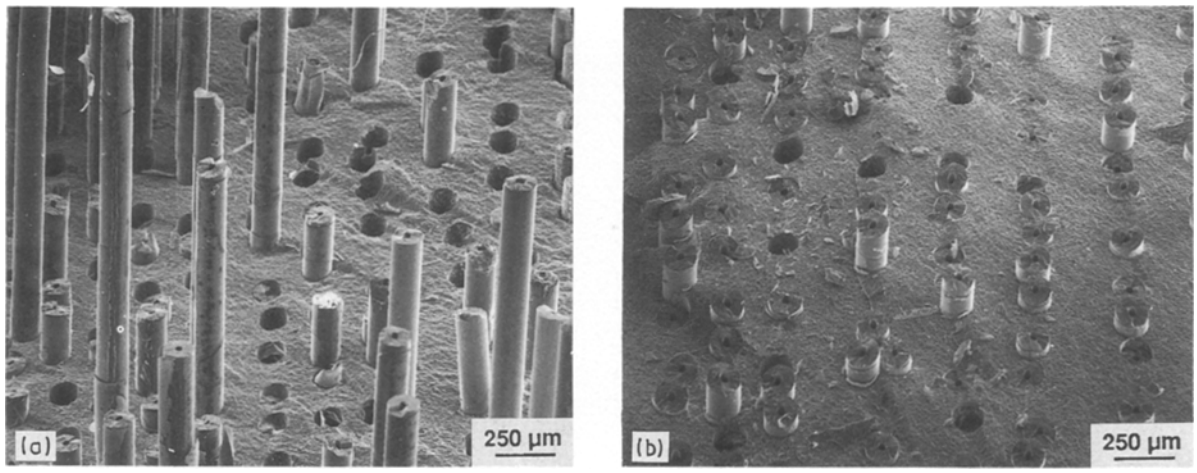


*Figure 8* SEM micrographs comparing the extent of fibre pullout observed after creep failure at (a) 70 MPa, $t_f$ = 794 h and (b) 150 MPa, $t_f$ = 34 h

(Fig. 8b), which was similar to the range of pullout lengths observed with monotonic tensile loading. The large fibre pullout lengths accompanying creep failure at 70 MPa indicates that interfacial shear strength decreases significantly during long duration creep of this composite system.

As shown in Fig. 9, pronounced separation along the fibre–matrix interface occurred in specimens which were crept at 70 Mpa. In some instances, the radial separation between the fibre and matrix approached 8 μm. Similar interfacial separation was not observed with specimens which had been crept at a higher stress level. The radial separation was approximately 2 to 3 μm larger than the separation which would be expected if complete loss of the carbon-rich fibre coating had occurred during creep (for example through reaction with oxide sintering aids during long term creep exposure). It is possible that radial contraction of the fibres during long-term creep contributed to the fibre–matrix separation which was observed. Investigation of the fibre ends after creep failure at 70 MPa showed two distinct types of fracture: flat fracture (characteristic of brittle failure), and rough, porous, fracture (see Fig. 10). Approximately 15% of the fibres had a rough fracture surface. The porous fibre fractures are thought to be the result of localized reaction between the fibres and sintering oxides which had not been completely dispersed. This mechanism is further verified by an experiment which involved exposing a sample for 800 h at 1350 °C without load; although not as severe, similar random degradation of the fibres was observed. Although speculative, it is possible that the rupture of fibres which were weakened by localized reaction with the sintering oxides could have been responsible for the discontinuous strain jumps which were observed during "steady-state" creep of the composite. Examination of the fibres also revealed that the 33 μm diameter carbon core of the SCS-6 fibres had completely oxidized. Since similar oxidation of the core was found after the short term exposure associated with the monotonic tensile tests, and was not observed after the 800 h zero-load experiment described above, oxidation of the fibre core most likely occurred *after* creep failure, during the approximately 15 min that it took for the furnace to cool after specimen failure.

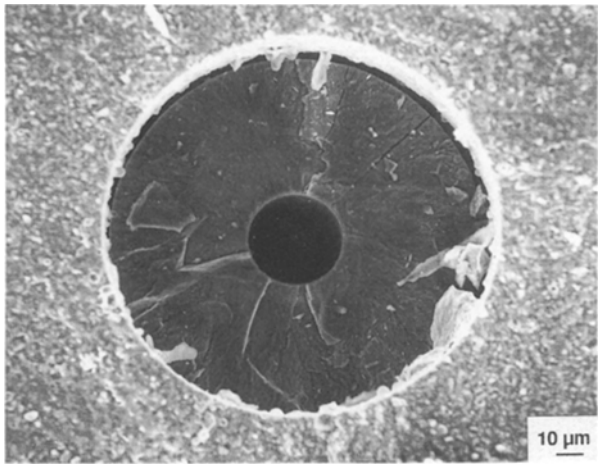


*Figure 9* SEM micrograph showing debonding along the fibre–matrix interface observed after creep failure at 70 MPa ($t_f$ = 794 h).

### 3.3. Comparison with hot-pressed $Si_3N_4$.

Kossowsky *et al.* [19] have investigated the tensile creep behaviour of monolithic $Si_3N_4$ at 1315 °C. The hot-pressed $Si_3N_4$ (HP-$Si_3N_4$) did not contain $Y_2O_3$; the major impurities were Ca, Al and Mg. When tested in air at a stress level of 69.7 MPa, the steady-state creep rate of the HP-$Si_3N_4$ was approximately $3.1 \times 10^{-6}\,s^{-1}$. For a similar stress, the average steady-state creep rate of the HP-$SiC_f$–$Si_3N_4$ composite, $2.5 \times 10^{-10}\,s^{-1}$, was approximately four orders of magnitude lower than the tensile creep rate of the HP-$Si_3N_4$ investigated by Kossowsky *et al.* [19] (see Fig. 6). Ferber *et al.* [23] have recently obtained data for the creep rate of an advanced 4 wt % $Y_2O_3$-$Si_3N_4$* processed by hot isostatic pressing (hereafter

*Grade NT-154, Norton Co., Massachusetts.

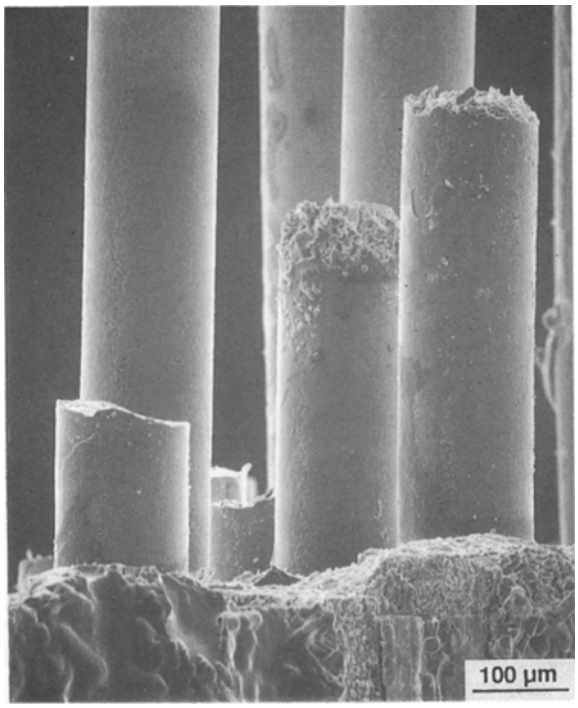


*Figure 10* SEM micrograph showing the two types of fibre fracture observed after creep failure at 70 MPa. The rough (porous) appearance of the two fibres on the right-hand side of the micrograph is attributed to the localized reaction of fibres with segregated sintering oxides. Approximately 15% of all fibres had a rough fracture surface, all other fibres showed a brittle failure mode (e.g., fibre on left-hand side of micrograph and in Fig. 9).

referred to as HIP-$Si_3N_4$). At a stress of 100 MPa and temperature of 1370 °C, the creep rate of the HIP-$Si_3N_4$ was approximately $4 \times 10^{-9}$ $s^{-1}$, which is similar to the creep rate of the composite at the slightly lower temperature of 1350 °C (Fig. 6).

As noted above, the HP-$Si_3N_4$ examined by Kossowsky *et al.* [19] did not contain $Y_2O_3$; whereas, the matrix of the HP-$SiC_f$–$Si_3N_4$ composite examined in the present investigation contained 5 wt % $Y_2O_3$. In creep tests conducted under three-point bending [4, 24] it has been shown that $Y_2O_3$ additions, in the range of 5 to 15 wt %, reduce the steady creep rate of monolithic $Si_3N_4$ by approximately one to two orders of magnitude. The reduction in creep rate obtained through $Y_2O_3$ additions is attributed to the formation of a more refractory grain boundary phase, which reduces the extent of grain boundary sliding [24]. Although $Y_2O_3$ additions are known to improve the creep resistance of hot-pressed $Si_3N_4$, MgO additions are detrimental [25]. The HP-$SiC_f$–$Si_3N_4$ examined in the present investigation had a MgO content of 1.25 wt %; thus, it is expected that further reductions in the creep rate of HP-$SiC_f$–$Si_3N_4$ composites can be achieved through changes in matrix composition (in particular through the substitution of other sintering aids for MgO). Also, the HP-$SiC_f$–$Si_3N_4$ composite was prepared by a dry-powder lay up process, which resulted in a very non-uniform fibre distribution (Fig. 1). Techniques which improve the uniformity in fibre distribution, such as tape casting, should further improve the creep resistance of $Si_3N_4$-based composites. Far more detailed microstructural investigations will be required to understand more completely how fibre and matrix damage evolves in fibre-reinforced ceramics during both short and long term creep exposure, and how this damage governs the observed creep behaviour. Preferably, these investigations should include a comparison of creep damage in inert and oxidizing environments.

## 4. Conclusions

The tensile creep behaviour of a unidirectional HP-$SiC_f$–$Si_3N_4$ composite was investigated in air at 1350 °C. The monotonic proportional limit of the composite was approximately 84 MPa. Based upon test results obtained for stress levels between 70 and 190 MPa the following conclusions can be made.

1. For stress levels of 70 to 150 MPa, an apparent steady-state creep was established. The steady-state creep rate ranged from an average of $2.5 \times 10^{-10}$ $s^{-1}$ at 70 MPa to $5.6 \times 10^{-8}$ $s^{-1}$ at 150 MPa. At 190 MPa only tertiary creep was observed. The "steady-state" creep rate of the composite, which contained 5.00% $Y_2O_3$ and 1.25% MgO as sintering aids, is comparable to the creep rate of monolithic $Si_3N_4$ containing 4 wt % $Y_2O_3$.
2. Over the limited range of stresses examined (70 to 190 MPa), no clear evidence of an acceleration in creep rate, beyond that which would be attributed to an increase in stress alone, was observed when the creep stress exceeded the monotonic proportional limit of the composite.
3. At 70 MPa, creep failure was accompanied by extensive fibre pullout and debonding along fibre matrix interfaces. The extent of fibre pullout diminished as the creep stress was increased. For specimens crept at 70 and 110 MPa, small discontinuous strain jumps were observed throughout the "steady-state" creep regime; these strain jumps are thought to result from the rupture of individual fibres which were degraded by reaction with the matrix oxides used to promote sintering.

## Acknowledgements

The author would like to thank Dr Jim DiCarlo (NASA Lewis Research Center) for discussions concerning the creep behaviour of SiC fibres. Discussions with Dr Sheldon Wiederhorn (National Institute of Standards and Technology) and Dr Matt Ferber (Oak Ridge National Laboratory) provided the author with valuable insight regarding the creep behaviour of monolithic $Si_3N_4$.

## References

1. F. ABBE, J. VINCENS and J. L. CHERMANT, *J. Mater. Sci. Lett.* **8** (1989) 1026.
2. S. DAPKUNUS, *Amer Ceram. Soc. Bull.*, **67** (1988) 389.
3. J. LANE, C. CARTER and R. DAVIS, *J. Amer. Ceram. Soc.* **71** (1988) 287.
4. R. F. PABST, in "Creep Behaviour of Crystalline Solids" edited by B. Wilshire and R. W. Evans, (Pineridge Press, Swansea, UK, 1985) p. 255.
5. S. M. WIEDERHORN and B. J. HOCKEY, "High Temperature Degradation of Structural Composites," presented at the

Seventh World Ceramics Congress, Montecatini Terme, Italy, June 24–30, 1990. Not published.
6. J. A. DICARLO, *J. Mater. Sci.* **21** (1986) 217.
7. J. A. DICARLO, "High Temperature Properties of CVD Silicon Carbide Fibers," presented at the International Conference on Whisker- and Fiber-Toughened Ceramics, Oak Ridge, TN, June 7–9, 1988.
8. ASTM Annual Book of Standards, Volume 3.01, (American Society for Testing and Materials, Philadelphia, 1988) p. 757.
9. J. W. HOLMES, T. KOTIL and W. T. FOULDS, in "Symposium on High Temperature Composites" (Technomic, Lancaster, PA, 1989) p. 176.
10. J. W. HOLMES, *J. Compos. Mater.* accepted for publication.
11. *Idem., J. Amer. Ceram. Soc.* in press.
12. K. M. PREWO, *J. Mater. Sci.* **23** (1988) 2475.
13. H. KODAMA, H. SAKAMOTO and T. MIYOSHI, *J. Amer. Ceram. Soc.* **72** (1989) 551.
14. O. SBAIZERO and A. G. EVANS, *ibid.* **69** (1986) 481.
15. D. B. MARSHALL and A. G. EVANS, *ibid.* **68** (1985) 225.
16. T. MAH, M. G. MENDIRATTA, A. P. KATZ, R. RUH and K. S. MAZDIYASNI, *ibid.*, **68** (1985) C248.
17. R. N. SINGH and A. R. GADDIPATI, *ibid.* **71** (1988) C100.
18. M. BARSOUM and O. Z. ZHOU, *Adv. Ceram. Mater.* **3** (1988) 361.
19. R. KOSSOWSKY, D. G. MILLER and E. S. DIAZ, *J. Mater. Sci.* **10** (1975) 983.
20. M. K. FERBER, M. G. JENKINS and V. J. TENNERY, *Ceram. Engng Sci. Proc.* **11** (1990) 1028.
21. R. M. ARONS and J. K. TIEN, *J. Mater. Sci.* **15** (1980) 2046.
22. B. J. HOCKEY, S. M. WIEDERHORN, W. LIU, J. G. BALDONI and S. T. BULJAN, "Tensile Creep of SiC Whisker Reinforced Silicon Nitride", presented at the Twenty-Seventh Automotive Technology Development Contractors Coordination Meeting (ATD/CCM), Detroit, MI, October 23–26, 1989. Not published.
23. M. K. FERBER, T. NOLAN, M. G. JENKINS, D. COFFEY and R. YECKLEY, presented at the 92nd Annual Meeting of the American Ceramic Society, Dallas, Texas, 1990. Not published.
24. S. UD DIN and P. S. NICHOLSON, *J. Mater. Sci.* **10** (1975) 1375.
25. P. J. DIXON-STUBBS and B. WILSHIRE, *J. Mater. Sci. Lett.* **14** (1979) 2773.

*Received 20 February*
*and accepted 16 July 1990*